Journal of Alloys and Compounds 623 (2015) 311–316

Contents lists available at ScienceDirect

Journal of Alloys and Compounds

journal homepage: www.elsevier.com/locate/jalcom

Study on the hydrogen storage and electrochemical properties of $Mm_{0.75}Mg_{0.25}Ni_{3.5}Co_{0.2}Al_x$ (x = 0.0–0.4) alloys

Lan Zhiqiang, Peng Wenqi, Fu Shuying, Wei Wenlou, Wei Ningyan, Guo Jin *

Guangxi Experiment Centre of Science and Technology, College of Physics Science and Technology, Guangxi University, Nanning 530004, China

ARTICLE INFO

Article history:
Received 24 June 2014
Received in revised form 9 October 2014
Accepted 20 October 2014
Available online 31 October 2014

Keywords:
Hydrogen storage alloy
Hydrogen storage property
Electrochemical property

ABSTRACT

$Mm_{0.75}Mg_{0.25}Ni_{3.5}Co_{0.2}Al_x$ (x = 0.0–0.4) alloys were prepared by the magnetic induction melting method. The influence of Al content on the hydrogen storage and electrochemical properties of the alloy was investigated. The results show that the hydrogen storage capacity is gradually reduced as the Al content increases. The (La,Pr,Nd)Ni_5 cell volume and the change of enthalpy also decrease as Al is added. Although the discharge capacity decreases with increasing Al content, the addition of Al can reduce the stability of $Mm_{0.75}Mg_{0.25}Ni_{3.5}Co_{0.2}Al_x$ (x = 0.0–0.4) hydride and improve the performance of hydrogen desorption thermodynamics. For the alloy electrode without Al, the maximum discharge capacity (C_{max}) and retention discharge capacity after 100 charge–discharge cycles (C_{100}) is 385 mA h g^{-1} and 202 mA h g^{-1}, respectively. For the alloy electrode with x = 0.4, while C_{max} is only 323 mA h g^{-1}, C100 is 273 mA h g^{-1}, which is much higher than that of the alloy without Al. The addition of Al can improve the charge–discharge cycle lifetime effectively and can increase the limiting current I_L. The kinetic performance of the $Mm_{0.75}Mg_{0.25}Ni_{3.5}Co_{0.2}Al_x$ (x = 0.0–0.4) alloy electrode can also be improved by increasing the Al content.

1. Introduction

Re–Mg–Ni-based hydrogen storage alloys have been attracted great attention as a negative electrode material due to their high energy density, long cycle life and high charge/discharge capacity [1–9]. For example, the effects of substitution of R(R = Zr or Nd) for La on the structure and electrochemical properties of the La–Mg–Ni hydrogen storage alloys have been investigated by Pan et al. [2,3]. In their studies, the electrochemical kinetics of the electrodes can be effectively improved by partial substitution of R(R = Zr or Nd) for La, in spite of the maximum discharge capacity of the alloy electrodes monotonously decreased as increasing the R(R = Zr or Nd) content. Liu et al. [4] have also investigated systematically the cycling behavior of the $La_{0.7}Mg_{0.3}Ni_{2.65-x}Co_{0.75}Mn_{0.1}Al_x$ (x = 0, 0.3) alloy electrodes, and they found that the formation of a dense Al oxide film during cycling was one of important factors for the improvement of the cycling stability of the La–Mg–Ni-based alloy electrodes with Al. Al is a valuable element in improving the cycle stability of the La–Mg–Ni-based alloys with the amount of Co reduced [5]. Balogun et al. [7] investigated that $LaNi_{4.2}Co_{0.3}Mn_{0.3}Al_{0.2}$, a single-phase alloy with hexagonal $CaCu_5$ type structure, presented the maximum discharge capacity of 330.4 mA h g^{-1}. Wang et al. [9] developed a Co-free $La_{0.8}Mg_{0.2}Ni_{3.4}Al_{0.1}$ alloy and found that the discharge capacity increased to 391.8 mA h g^{-1} after surface was modified with polyaniline, compared to 382.5 mA h g^{-1} for the bare alloys. Although the La–Mg–Ni-based alloy has a high hydrogen storage capacity, the cyclic durability of this type alloy is not so satisfied for practical applications. Co is a key element for improving charge–discharge cyclic stability in La–Mg–Ni-based alloys [10], but the charge–discharge capacity and the kinetic properties are degraded as the Co content increases [11]. Therefore, how to improve the comprehensive electrochemical properties of low-Co Re–Mg–Ni-based hydrogen storage alloys is a topic worth investigating. Gao et al. [12] researched the $La_{0.8-x}Gd_{0.2}Mg_xNi_{3.1}Co_{0.3}Al_{0.1}$($x$ = 0.1–0.5) alloys and found that the chemical composition and crystalline phase structure of these alloys closely depended on the Mg content (x). It showed that the cycle stability was improved dramatically for x = 0.15. However, both the cyclic stability and discharge capacity of the alloy electrodes decrease as the Mg content further increases. Chen et al. [13] investigated electrochemical properties of $La_{0.78}Ce_{0.22}Ni_{3.73}Mn_{0.30}Al_{0.17}Fe_xCo_{0.8-x}$ (x = 0, 0.2, 0.5, 0.8) alloys and found that the discharge capacity and high rate discharge ability were weaken as increasing Fe content. Here, in order to investigate the effect of Al element on the comprehensive properties of

* Corresponding author.
E-mail address: guojin@gxu.edu.cn (G. Jin).

http://dx.doi.org/10.1016/j.jallcom.2014.10.097
0925-8388/

the low-Co Re–Mg–Ni alloy, the $Mm_{0.75}Mg_{0.25}Ni_{3.5}Co_{0.2}Al_x$ (x = 0.0–0.4) alloys were prepared by magnetic levitation melting under argon atmosphere, and then hydrogen storage and electrochemical properties were discussed in detail.

2. Experimental

The $Mm_{0.75}Mg_{0.25}Ni_{3.5}Co_{0.2}Al_x$ (x = 0.0–0.4) alloys were prepared by magnetic levitation melting under an argon atmosphere. The La-rich mischmetal (Mm) used in this work contained La85.2%, Ce3.3%, Pr2.6% and Nd8.9%. The purity of La, Ce, Pr, Nd, Mg, Ni and Co was above 99.9 wt%. The ingots were turned over and remelted three times to ensure good homogeneity, and then part of the alloys were mechanically crushed and ground into 200 mesh powders for the experiments. The crystal structures of the samples were characterized using a Rigaku D/max 2500 V diffractometer. For scanning electron microscope (SEM) analysis, the sample was encapsulated in epoxy resin for polishing, and then the polished surface was etched with a 60% HF aqueous solution. The morphology and elemental composition of the ingot samples were investigated using an SU-8020/X-MAX80 Field Emission Scanning Microscope equipped with an Energy Dispersive Spectrometer (EDS). All the electrodes were prepared by mixing the alloy powder with carbonyl nickel powder in a weight ratio of 1:4 and then cold-pressed under a pressure of 20 MPa into a pellet of 10 mm diameter and about 1 mm thickness.

Electrochemical measurements were performed at room temperature in a tri-electrode open cell. $NiOOH/Ni(OH)_2$ was adopted as the counter electrode, the Hg/HgO was adopted as a reference electrode and 6 mol L^{-1} KOH solution was used as the electrolyte. For activation and charge/discharge cycling, all the alloy electrodes were measured by a DC-5 battery testing instrument at a 100 mA g^{-1} charge rate for 5 h, followed by a 10 min rest and then discharged at an 80 mA g^{-1} discharge rate to a cut-off cell potential of −0.5 V relative to the Hg/HgO reference electrode.

The electrochemical characteristics of the $Mm_{0.75}Mg_{0.25}Ni_{3.5}Co_{0.2}Al_x$ (x = 0.0–0.4) alloy electrodes were investigated in the following procedures. The high rate discharge (*HRD*) was tested on an automatic Arbin-BT2000 battery-testing instrument. The linear polarization and the Tafel polarization were carried out on the GAMRY Corrosion Electrochemical Measurement System. A scanning rate of 10 mV s^{-1} was used from −0.3 to 1.0 V for the Tafel curve. The hydrogen diffusion coefficients were measured by means of the constant potential step discharge technique. The test electrodes in a fully charged state were discharged at a constant potential step of −600 mV for 7200 s.

3. Results and discussion

3.1. Microstructure

Fig. 1 shows the XRD patterns of the $Mm_{0.75}Mg_{0.25}Ni_{3.5}Co_{0.2}Al_x$ (x = 0.0–0.4) alloys. It can be seen that all of the alloys mainly contain (La,Pr,Nd)Ni_5 with a hexagonal $CaCu_5$-type structure and $LaMg_2Ni_9$ with a $PuNi_3$-type structure phase. Another $CaCu_5$-type structure $LaAlNi_4$ phase appears as the Al content increases. The lattice parameters of (La,Pr,Nd)Ni_5, $LaMg_2Ni_9$ and $LaAlNi_4$, calculated from the XRD data by Jade 6.0 software, are listed in Table 1.

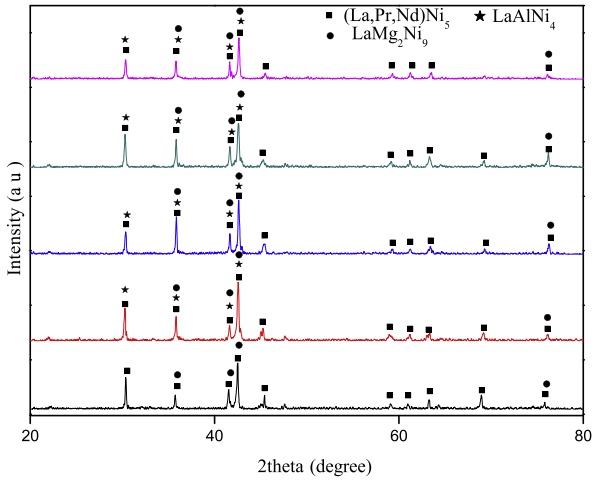

Fig. 1. XRD patterns of the $Mm_{0.75}Mg_{0.25}Ni_{3.5}Co_{0.2}Al_x$ (x = 0.0–0.4) alloys.

As shown in Table 1, the cell volumes of the (La,Pr,Nd)Ni_5 and $LaMg_2Ni_9$ phase decrease as Al is added. The cell volume of the (La,Pr,Nd)Ni_5 phase decreases from 86.98 $Å^3$ to 86.11 $Å^3$ as the x value increases from 0.0 to 0.4, while the cell volume of the $LaAlNi_4$ phase first decreases from 90.14 $Å^3$ to 90.07 $Å^3$ as the x value increases from 0.1 to 0.3, and then increases to 90.19 $Å^3$ as the x value further increases to 0.4.

Fig. 2a shows the SEM image for the as-cast $Mm_{0.75}Mg_{0.25}Ni_{3.5}Co_{0.2}Al_{0.1}$ alloy as a representative example of $Mm_{0.75}Mg_{0.25}Ni_{3.5}Co_{0.2}Al_x$ (x = 0.0–0.4) alloys. The element composition of the alloy is identified by EDS, and the result is illustrated in Fig. 2b and c. EDS (Fig. 2b) analysis for region A (the dark region in Fig. 2a) shows an atomic ratio of 8.86La, 16.5 Mg and 68.45Ni, which is close to the ideal atomic ratio of 8.33La, 16.67 Mg and 75Ni for the $LaMg_2Ni_9$ phase. According to EDS and XRD analysis, region A should be the $LaMg_2Ni_9$ phase. Region B (the gray region in Fig. 2a) corresponds to the $CaCu_5$-type structure of the (La,Pr,Nd)Ni_5 and $LaAlNi_4$ phases. The abundances of all elements in the alloy agree well with the expected values.

In terms of the phase structure of the alloy, $LaMg_2Ni_9$ is one of the three main phases in the $Mm_{0.75}Mg_{0.25}Ni_{3.5}Co_{0.2}Al_x$ (x = 0.0–0.4) alloys. However, the hydrogen storage capacity of $LaMg_2Ni_9$ is only about 0.33 wt% H/M [14], which is much lower than that of the $CaCu_5$-type structure. Therefore, only the (La,Pr,Nd)Ni_5 and $LaAlNi_4$ phases are considered as the main hydrogen storage phase in the $Mm_{0.75}Mg_{0.25}Ni_{3.5}Co_{0.2}Al_x$ (x = 0.0–0.4) alloys.

3.2. Hydrogen storage properties

The PCT curves of the $Mm_{0.75}Mg_{0.25}Ni_{3.5}Co_{0.2}Al_x$ (x = 0.0–0.4) alloys at different temperatures are shown in Fig. 3. It can be seen that the hydrogen storage capacity and the plateau pressure of the alloys decrease with increasing Al content. It is well known that hydrogen atoms mainly occupy empty sites in hydrogen storage in a bulk alloy. Therefore, the shrinkage of the (La,Pr,Nd)Ni_5 cell volume may result in a decrease in the hydrogen storage capacity of the $Mm_{0.75}Mg_{0.25}Ni_{3.5}Co_{0.2}Al_x$ (x = 0.0–0.4) alloy. According to the PCI curves shown in Fig. 3, and based on the Van't Hoff equation $\ln P = \frac{\Delta H}{RT} - \frac{\Delta S}{R}$, the Van't Hoff plots are shown in Fig. 4. The change of enthalpy, ΔH, is calculated from the linear slope in Fig. 4 and is given in Table 2. The results show that ΔH is −25.17 kJ mol^{-1}, −23.38 kJ mol^{-1}, −19.68 kJ mol^{-1}, −22.18 kJ mol^{-1} and −21.12 kJ mol^{-1} for x = 0.0, 0.1, 0.2, 0.3 and 0.4, respectively. It is interesting to note that the value of ΔH decreases as Al is added, which indicates that the addition of Al reduces the stability of the $Mm_{0.75}Mg_{0.25}Ni_{3.5}Co_{0.2}Al_x$ (x = 0.0–0.4) hydride. This means that

Table 1
The lattice parameters of the $Mm_{0.75}Mg_{0.25}Ni_{3.5}Co_{0.2}Al_x$ (x = 0.0–0.4) alloys.

Samples	Phase	Lattice parameter		Cell volume ($Å^3$)
		a (Å)	c (Å)	
x = 0.0	(La,Pr,Nd)Ni_5	5.015	3.993	86.98
	$LaMg_2Ni_9$	4.993	24.17	521.9
x = 0.1	(La,Pr,Nd)Ni_5	5.024	3.991	86.55
	$LaAlNi_4$	5.060	4.066	90.14
	$LaMg_2Ni_9$	4.983	24.16	519.5
x = 0.2	(La,Pr,Nd)Ni_5	5.017	3.970	86.54
	$LaAlNi_4$	5.060	4.062	90.08
	$LaMg_2Ni_9$	4.990	24.10	519.6
x = 0.3	(La,Pr,Nd)Ni_5	4.995	3.992	86.26
	$LaAlNi_4$	5.079	4.059	90.07
	$LaMg_2Ni_9$	5.000	24.01	519.9
x = 0.4	(La,Pr,Nd)Ni_5	4.996	3.983	86.11
	$LaAlNi_4$	5.062	4.064	90.19
	$LaMg_2Ni_9$	4.987	24.08	518.8